The AAPS Journal, Vol. 19, No. 2, March 2017 (© 2017)
DOI: 10.1208/s12248-016-0034-8

Research Article

Theme: Recent Advances in Musculoskeletal Tissue Engineering
Guest Editor: Aliasger K. Salem

A Comparative Study of the Bone Regenerative Effect of Chemically Modified RNA Encoding BMP-2 or BMP-9

Behnoush Khorsand,[1] Satheesh Elangovan,[2,5] Liu Hong,[3] Alexander Dewerth,[4] Michael S. D. Kormann,[4] and Aliasger K. Salem[1,2,5]

Received 25 October 2016; accepted 20 December 2016; published online 10 January 2017

Abstract. Employing cost-effective biomaterials to deliver chemically modified ribonucleic acid (cmRNA) in a controlled manner addresses the high cost, safety concerns, and lower transfection efficiency that exist with protein and gene therapeutic approaches. By eliminating the need for nuclear entry, cmRNA therapeutics can potentially overcome the lower transfection efficiencies associated with non-viral gene delivery systems. Here, we investigated the osteogenic potential of cmRNA-encoding BMP-9, in comparison to cmRNA-encoding BMP-2. Polyethylenimine (PEI) was used as a vector to increase *in vitro* transfection efficacy. Complexes of PEI-cmRNA (encoding BMP-2 or BMP-9) were fabricated at an amine (N) to phosphate (P) ratio of 10 and characterized for transfection efficacy *in vitro* using human bone marrow stromal cells (BMSCs). The osteogenic potential of BMSCs treated with these complexes was determined by evaluating the expression of bone-specific genes as well as through the detection of bone matrix deposition. It was found that alkaline phosphatase (ALP) expression 3 days post transfection in the group treated with *BMP-9*-cmRNA was significantly higher than that in the group that received *BMP-2*-cmRNA treatment. Alizarin red staining and atomic absorption spectroscopy demonstrated enhanced osteogenic differentiation as evidenced by increased bone matrix production by the BMSCs treated with *BMP-9*-cmRNA when compared to cells treated with *BMP-2*-cmRNA. *In vivo* studies showed increased bone formation in calvarial defects treated with the *BMP-9*-cmRNA and *BMP-2*-cmRNA collagen scaffolds when compared to empty defects. The connectivity density of the regenerated bone was higher (2-fold-higher) in the group that received *BMP-9*-cmRNA compared to *BMP-2*-cmRNA. Together, these findings suggest that cmRNA-activated matrix encoding osteogenic molecules can provide a powerful strategy for bone regeneration with significant clinical translational potential.

KEY WORDS: bone regeneration; bone morphogenetic protein-2; chemically modified RNA; gene delivery; signaling pathways.

INTRODUCTION

Trauma or diseases such as osteoporosis which results in bone loss are responsible for a large portion of healthcare expenses in the world. For example, approximately 10 million osteoporotic fractures occur annually among adults 50 years of age or older in the USA alone (1), which costs over 14 billion dollars in medication (2). Therefore, there is an enormous demand in both medicine and dentistry for bone repair or replacement in cases such as joint and spinal arthrodesis as well as in cranio-maxillofacial surgery. Bone is one of the few organs that maintains its potential for natural repair and regeneration of minor fractures into adulthood. However, the absence of adequate union in critical-sized defects prevents the damaged bone from being restored to its original functionality (3). Thus, various strategies such as tissue engineering have been developed to improve bone repair and regeneration for the treatment of severe fractures. In practice, recombinant protein-based strategies are one of

[1] Division of Pharmaceutics and Translational Therapeutics, University of Iowa College of Pharmacy, Iowa City, Iowa, USA.
[2] Department of Periodontics, University of Iowa College of Dentistry, Iowa City, Iowa, USA.
[3] Department of Prosthodontics, University of Iowa College of Dentistry, Iowa City, Iowa, USA.
[4] Department of Pediatrics (Section I), Translational Genomics and Gene Therapy, University of Tübingen, Wilhelmstr. 27, 72074, Tübingen, Germany.
[5] To whom correspondence should be addressed. (e-mail: satheeshelangovan@uiowa.edu; aliasger-salem@uiowa.edu)

the most successful approaches that have shown great efficacy in the clinic. Bone morphogenetic proteins (BMPs) are members of the transforming growth factor-β (TGF-β) superfamily, and, to date, more than 20 BMP family members have been recognized. These factors mediate signaling pathways that promote osteoblast differentiation from mesenchymal stem cell (MSC) precursors during skeletal development and bone formation (4). Comparative studies investigating all BMPs have confirmed their different biological activities, and among these BMP family members BMP-2, BMP-4, BMP-6, and BMP-9 are well recognized as having vital roles in ossification (4,5). Although recombinant human BMP-2 (rhBMP-2) has been extensively studied and has demonstrated successful bone healing and osteoregenerative effects in clinical applications (6–9), it is uncertain if it is the most potent osteogenic factor among the BMPs. There are several studies that have shown that BMP-9 has stronger osteogenic potential compared to BMP-2 (4,10).

BMPs initiate their signaling by binding to two types of heterodimeric complex of transmembrane serine/threonine kinase receptors, type I BMP (ALK1, ALK2, ALK3, ALK4, and ALK6) and type II (BMPRI, ActRIIA, and ActRIIB) (11,12). Upon binding of BMPs to their receptors and formation of heterotetrameric complex, the activated receptor kinases phosphorylate downstream transcription factors, known as Smads (Smad 1/5/8). The phosphorylated Smads in association with Smad 4 form a complex which then translocates to the nucleus and subsequently activates the expression of osteogenic genes such as alkaline phosphatase (ALP), osteocalcin, and runt-related transcription factor 2 (Runx-2) (13). BMPs can also signal through a Smad-independent mitogen-activated protein kinase (MAPK) pathway. BMP-MAPKs transduce their signaling cascade into nuclei *via* JNK-1, ERK1/2, and p38 pathways where they upregulate the expression of osteogenic genes (11) (Fig. 1). BMP-2 plays an important role in osteoblast maturation and differentiation from MSCs mostly through activating the Smad signaling pathway and upregulating targeted osteogenic genes (5). BMP-9, which is also known as growth differentiation factor 2, can promote the differentiation of osteoblasts from MSCs both *in vitro* and *in vivo* (4,14,15); however, the specific mechanism responsible for BMP-9-mediated osteogenesis remains to be elucidated. Many signaling pathways have been found to be involved in BMP-9-mediated osteogenesis. Their signaling pathways are unique but likely overlap with other osteogenic members of the BMP family to the some extent. Like other osteogenic BMPs, BMP-9 signals through the Smad signaling pathway, however, noggin which is an extracellular antagonist does not inhibit BMP-9 signal transduction as it does with other BMPs (16). Also within the BMP-Smad signaling pathway, BMP-9 mediates signal transduction through ALK1 and ALK2, while BMP-2 preferentially binds to ALK3 and ALK6 and recruits type II receptors (17,18). BMP-9 signaling also crosstalks with other signaling pathways such as the TGF-β1 pathway, Wnt/β-catenin signaling pathways, insulin-like growth factor (IGF) pathways, growth hormone (GH) pathway, and MAPKs signaling pathways, which play a critical role during the process of BMP-9-mediated osteogenesis (19) (Fig. 1). Moreover, it has been shown that BMP-3, which has inhibitory effects on BMP-2-mediated bone formation, does not inhibit BMP-9-mediated osteogenesis (4). These results suggest that BMP-9 exhibits unique signaling to bypass BMP negative regulators of the downsteam genes in MSCs, which in turn induces bone formation.

Despite their great therapeutic potential, major drawbacks with local recombinant human protein therapy include their high cost as well as their short half-lives. Their low bioavailability *in vivo* is often the reason for supraphysiological dosage administration in an effort to achieve successful therapy (20), which has been associated with several side effects such as a higher cancer risk (21). There are alternative approaches to overcome these limitations including non-viral gene therapy. Recently, utilization of chemically modified messenger RNA (cmRNA), as opposed to plasmid DNA (pDNA), has gained substantial attention (22,23). In our recent study, we have shown the superiority of cmRNA-encoding BMP-2 compared to pDNA-encoding BMP-2 in terms of bone regeneration efficacy (22). It has been shown that cmRNA is a promising means for many therapeutics due to its high stability and low immunogenicity (24,25). The cmRNA translational efficacy is also higher than DNA alternatives since it bypasses the need for nuclear trafficking and is therefore immediately translated once it has entered the cytoplasm. The use of cmRNA also abrogates the risk of integration to the host genome. To date, the strong osteogenic potential of BMP-9 has been demonstrated using adenoviral gene transduction (4) and rhBMP-9 protein (10).

Here, we investigate the osteogenic potential and bone regeneration capacity of cmRNA-encoding *BMP-9* in comparison to cmRNA-encoding *BMP-2* in bone marrow stromal cells (BMSCs) (*in vitro*) and *in vivo*. We found that *BMP-9*-cmRNA demonstrated significantly higher ALP expression, higher alizarin red staining, as well as higher calcium production when compared to *BMP-2*-cmRNA. Moreover, collagen scaffolds loaded with *BMP-9*-cmRNA showed a 2-fold increase in connectivity density of the regenerated bone when implanted into rat calvarial defect sites compared to groups treated with *BMP-2*-cmRNA.

MATERIALS AND METHODS

Materials

Branched PEI (mol. wt. 25 kDa) and the GenElute™ HP endotoxin-free plasmid maxiprep kit were purchased from Sigma-Aldrich® (St. Louis, MO). Human bone marrow stromal cells (BMSCs) were purchased from American Type Culture Collection (ATCC®, Manassas, VA). Dulbecco's Modified Eagle's Medium (DMEM), trypsin-EDTA (0.25%, 1× solution), and Dulbecco's phosphate buffered saline (PBS) were purchased from Gibco® (Invitrogen™, Grand Island, NY). Fetal bovine serum (FBS) was obtained from Atlanta Biologicals® (Lawrenceville, GA). Gentamycin sulfate (50 mg/ml) was purchased from Mediatech Inc. (Manassas, VA). The RNA-easy kit was purchased from Qiagen Inc. The TaqMan Reverse Transcription Reagents and 18S-rRNA

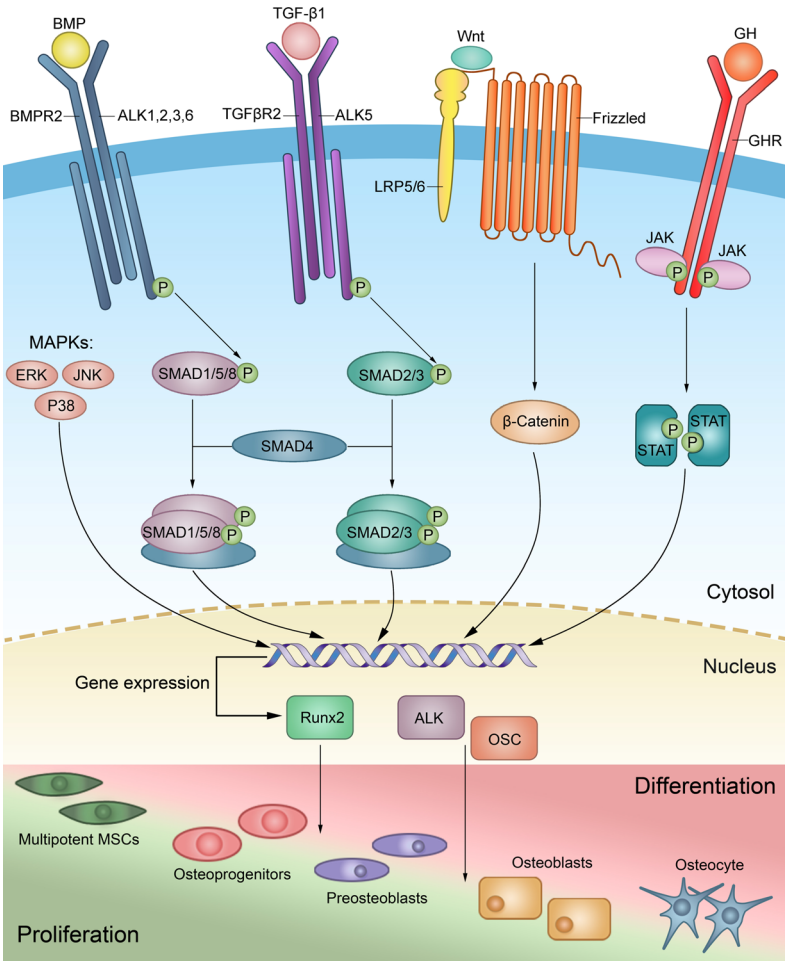

Fig. 1. Schematic illustration of the main BMP signaling pathways involved in the differentiation of mesenchymal stem cells into osteocytes. BMP-2 mediates osteogenesis mainly through SMADs and MAPK pathways. BMP-9 not only induces osteogenic differentiation of MSCs through SMAD and MAPK pathways but also initiates several signaling cascades and crosstalk with various other pathways

were purchased from Applied Biosystems (Foster City, CA). The absorbable type-I bovine 3-dimensional collagen scaffold was purchased from Zimmer Dental Inc. (Carlsbad, CA). All other chemicals and solvents used were of reagent grade.

Methods

Bone Marrow Stromal Cells (BMSCs)

BMSCs were maintained in DMEM (supplemented with 10% FBS and 1% gentamycin (50 μg/ml)) in a humidified incubator (Sanyo Scientific Autoflow, IR direct heat CO_2 incubator) at 37°C and 5% CO_2. In this study, BMSCs were used from passage 3 to passage 4. Cells were cultured on 75 cm^2 polystyrene cell culture flasks (Corning, NY, USA).

Generation of Chemically Modified RNA (cmRNA) Encoding BMP-2 and BMP-9

Chemically modified RNA encoding BMP-2 and BMP-9 were prepared following our previously reported protocol (22). In brief, complementary DNA (cDNA) encoding *BMP-2* or *BMP-9* was subcloned into a PolyA-120 containing T7 pVAX1 (Life Technologies, Madison, WI) and linearized with XbaI. Plasmid purity was examined spectrophotometrically. Subsequently, mRNA encoding-BMP-2 or BMP-9 was synthesized using the MEGAscript T7 Transcription Kits (Life Technologies, Madison, WI) and capped with the anti-reverse cap analog (*ARCA; 7-methyl (3'-O-methyl) GpppGm7G (5') ppp (5') G*). Modified ribonucleic acid triphosphates were added to the reaction in the form of pseudouridine-5'-triphosphate and 5-methylcytidine-5'-triphosphate (*Ψ (1.0) m5C (1.0)*) at a ratio of 100%; to achieve mRNA modification.

Complex Fabrication and Characterization

For all of the *in vitro* studies, cmRNA-encoding BMP-2 or BMP-9 was delivered using PEI as a cationic vector. Fabrication of PEI-cmRNA complexes was performed as described previously (22). Briefly, complexes were fabricated at amine (N) to phosphate (P) ratio of 10, in order to achieve optimal transfection efficacies (26). Complexes were prepared by adding PEI solution (500 μL) to cmRNA solution (500 μL) containing 50 μg cmRNA (encoding BMP-2 or BMP-9) and

vortexed for 30 s, followed by incubation at room temperature for 30 min. The final volume of the complexes utilized for *in vitro* experiments was 20 μl, containing 1 μg cmRNA.

Complexes were characterized for their size and zeta-potential using a Zetasizer Nano-ZS (Malvern Instruments, Westborough, MA). Using 10-mm diameter cells, the particle size and particle size distribution were measured by photon correlation spectroscopy (PCS), using dynamic laser light scattering (4 mW He–Ne laser with a fixed wavelength of 633 nm, 173° backscatter at 25°C). Using the same instrument, Zeta potentials of the complexes in water were assessed *via* folded capillary cells. Zeta potential measurements were performed by the laser scattering method (Laser Doppler Micro-electrophoresis, He–Ne laser, 633 nm, and 17° light scatter at 25°C). All measurements were performed in triplicate.

Fabrication of cmRNA-Embedded Collagen Scaffolds

The collagen scaffolds were hand cut into 5×2 mm cylinder. Then, the treatments were injected into the collagen scaffolds using a sterile 28 gage needle. Afterwards, the cmRNA-embedded collagen scaffolds were freeze-dried for subsequent use.

In Vitro Osteoblastic Gene Expression

Using real-time PCR, osteogenic stimulation of BMSCs in the presence of cmRNA-encoding BMP-9 or BMP-2 was investigated. Expression of osteocalcin (OSC), Runx-2 and ALP, was examined 3 days post transfection. RNeasy Mini Kit (Qiagen, Valencia, CA, USA) was utilized to extract total RNA from isolated cells. Total RNA was reverse transcribed to generate Complementary DNA (cDNA) with TaqMan Reverse Transcription Reagents. The PCR reactions were carried out in a PTC-200 Peltier Thermal Cycler (MJ Research, BioRad, Walthan, MA, USA). 18S Ribosomal RNA (18S-rRNA) was used as housekeeping gene as a control (Undisclosed sequences, Applied Biosystems, Foster City, CA). Quantitative real-time PCR (Q-RT-PCR) reactions were completed in a 7300 real-time PCR system (Applied Biosystems, Foster City, CA), and transcription of OSC, Runx-2, and ALP were quantified. The gene expression were reported relative to untreated controls using the relative quantitation using comparative C_T ($2^{-\Delta\Delta CT}$) method.

Quantitative and Qualitative Detection of Calcium Deposition

The calcium content was assessed quantitatively and qualitatively, by means of atomic absorption spectroscopy (AAS) and alizarin red staining, respectively.

Quantitative measurements by chemical analysis were carried out on a PerkinElmer model 2380 atomic absorption spectrometer. In the absorption mode for the calcium (wavelength of 422.7 nm), using an air-acetylene flame, Ca^{2+} ion concentration was quantified as previously described (22). In brief, 14 days post transfection, BMSCs were hydrolyzed by incubating them with HCL (0.6 N) overnight. The AAS samples were prepared by mixing hydrolyzed samples (450 μL) with 2.5% lanthanum oxide in 0.6 N HCl (550 μL). Commercial calcium standards were utilized to calibrate the spectrophotometer. The results were normalized to the untreated controls.

Extracellular mineralization was qualitatively evaluated by alizarin red staining, 14 days after adding the treatments. Samples were fixed in formalin (10%) for 10 min and washed with distilled water for several times afterwards. Then, fixed samples were incubated with alizarin red solution (2%) for 10 min. Following extensive washing with distilled water (until no additional alizarin red continued to leak into the solution), the samples were imaged with the Nikon TE-300 inverted microscope.

Animals and Surgical Procedure

All animal experimental procedures were approved by the University of Iowa Institutional Animal Care and Use Committee, Iowa. Fourteen weeks old Fisher (CDF®) male white rats (F344/DuCrl, 250 g) were purchased from Harlan Laboratories (Indianapolis, IN) and housed and cared for in the animal facilities. The animals were anesthetized by intraperitoneal injection with a mixture of ketamine (80 mg/kg) and xylazine (8 mg/kg). Using a sterile instrument and aseptic technique, a sagittal incision was made and the subcutaneous tissue, musculature, and periosteum were reflected using a blunt dissection to expose the calvarium. Critical-sized defects (5-mm diameter) were generated on the calvarium using a round carbide bur. The defects were randomly allocated into the two following treatment groups: 1) *BMP-2*-cmRNA-loaded scaffolds ($n = 6$) and 2) *BMP-9*-cmRNA-loaded scaffolds ($n = 6$). Empty defect ($n = 6$) was used as controls. The scaffold sizes were adjusted to the diameter and thickness of the defects and implanted into the defects for 4 weeks. The periosteum and skin were repositioned and closed in layers using sterile silk sutures. Post surgery, each animal received an intramuscular injection of buprenorphine (0.15 mg), as an analgesic. The animals were carefully monitored daily for 5 days during postoperative recovery. After 4 weeks, all animals were euthanized by CO_2 inhalation and the calvarial defect sites with surrounding bone were dissected and fixed in neutral buffered formalin (10%) for subsequent evaluation.

Micro-CT Analysis of the Regenerated Bone

Bone volume and connectivity density were quantified using a cone-beam micro-CT 40, Scanco Medical AG (Switzerland). Using three dimensional X-ray micro-CT imaging system, defects were scanned in 70% ethanol (55 kVp, 145 μA with a voxel size of 10 μm, 300 ms exposure). Computer analysis was performed using a constant 3.5-mm diameter circular region of interest, and the percent of bone volume and connectivity density in the defect site were calculated as described previously (22).

Histological Observation

After micro-CT analysis, fixed bone samples were subjected to decalcification (Surgipath, Decalcifier II). Upon obtaining a negative test for the presence of calcium, fixed

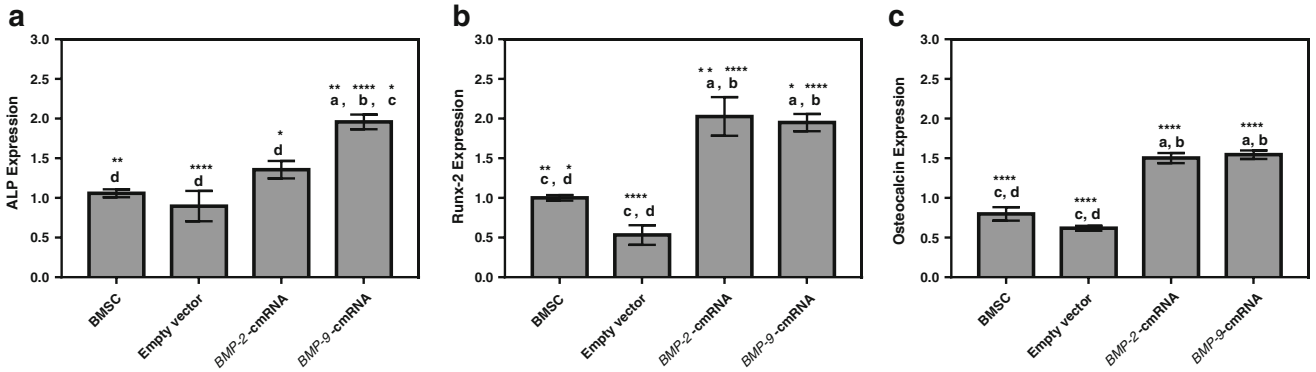

Fig. 2. Using real-time PCR, the expression level of genes encoding **a** ALP, **b** Runx-2, and **c** Osteocalcin in BMSCs treated with empty vectors, *BMP-2*-cmRNA nanoplexes, or *BMP-9*-cmRNA nanoplexes (prepared at an N:P ratio of 10, ($n = 4$)) 3 days post transfection was determined. Significant differences between the treatments and the untreated controls were evaluated by one way ANOVA followed by Tukey's post-test. *a* statistically significant difference from BMSC, *b* statistically significant difference from empty vector, *c* statistically significant difference from *BMP-2*-cmRNA, and *d* statistically significant difference from *BMP-9*-cmRNA (****$p < 0.0001$; **$p < 0.01$; *$p < 0.1$). Values are expressed as mean ± SEM

specimens were dehydrated using gradually increasing concentrations of ethanol followed by treatment with xylene (Merck, Germany) and embedded in paraffin. Cross-sections of 5-μm thickness in the central portion of the rat bone specimens were collected on Superfrost Plus slides (Fisher Scientific®), deparaffinized, and stained with Harris hematoxylin and eosin (H & E staining). The central area of the defect was assessed for newly formed bone using a bright field microscope (Olympus Stereoscope SZX12). Histomorphometry of the newly formed bone tissue was performed using the Image J software for image analysis.

Data Presentation and Statistical Analysis

Statistical analyses were performed using the GraphPad Prism version 7.00 (GraphPad Software, CA, USA). All experiments were performed at least in triplicate, and obtained values are reported as mean ± SEM. One-way ANOVA followed by Tukey's multiple comparisons test was performed to analyze comparison of multiple groups. Non-parametric Kruskal–Wallis test with Dunnett's post-test analysis was performed for comparing all pairs of treatments. P values ≤ 0.05 were considered statistically significant.

RESULTS AND DISCUSSION

Complex Formation and Characterization

PEI was used as a vector to aid the *in vitro* cellular transfection in order to achieve higher transfection efficiency. cmRNA was incorporated into PEI to form complexes at an N/P ratio of 10:1. The size of complexes ranged from 70 to 90 nm with a narrow size distribution and the average polydispersity index (PDI) less than 0.2. The zeta potential of the complexes was in the range of +33 to +45 mV.

Enhancement of Osteoblastic Gene Expression in the Presence of BMP-9-cmRNA and BMP-2-cmRNA Complexes

As discussed in the introduction, BMP-2 and BMP-9 promote osteogenesis by activating several signaling cascades such as Smad-dependent and Smad-independent (*e.g.*, MAPK) pathways leading to expression of osteogenic factors such as Runx2, ALP, and OSC, subsequently inducing osteoblastic differentiation (27). In the current study, it was observed that cmRNA-encoding BMP-2 and BMP-9 with the aid of vectors were able to successfully transfect the BMSCs *in vitro*. Adequate amounts of BMP-2 and BMP-9 secretion

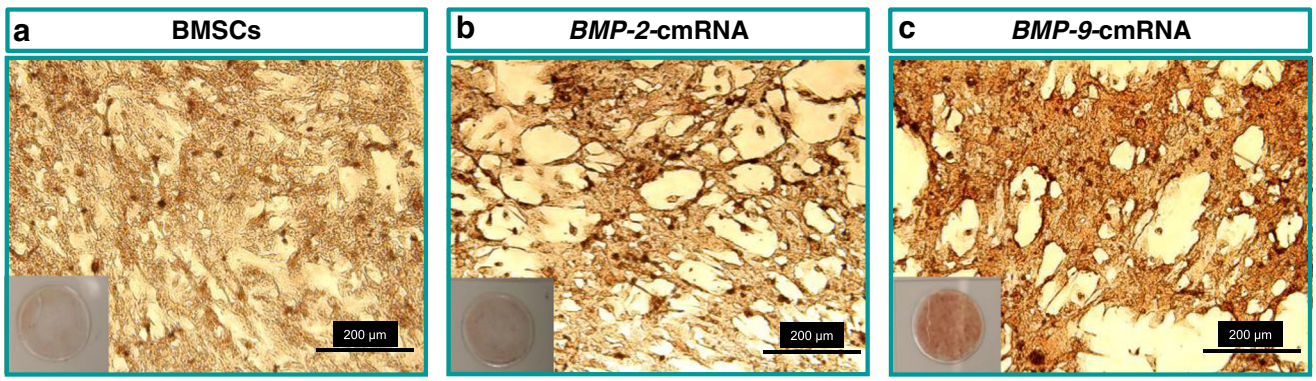

Fig. 3. Visual representation of alizarin red stained BMSCs, 14 days post transfection. **a** BMSCs untreated control, **b** *BMP-2*-cmRNA nanoplexes transfected BMSCs, and **c** *BMP-9*-cmRNA nanoplexes transfected BMSCs. *Scale bar* 200 μm

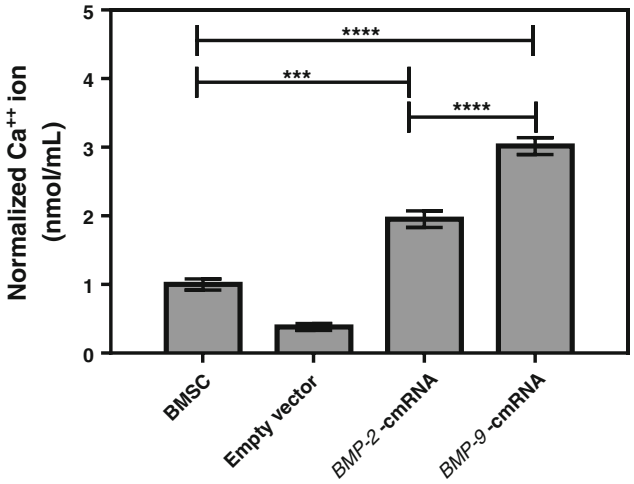

Fig. 4. Calcium mineralization levels were determined using atomic absorption spectroscopy on BMSC suspensions 14 days post transfection with indicated treatment ($n = 8$)). Significant differences between the treatments and the untreated controls were evaluated by one way ANOVA followed by Tukey's post-test (****$p < 0.0001$, ***$p < 0.001$). Values are expressed as mean ± SEM

upon transfection resulted in the subsequent expression of all investigated osteogenic markers including early (ALP and Runx2) and late (osteocalcin) markers (Fig. 2). Figure 2a demonstrates the ALP expression of BMSCs transfected with BMP-2 and BMP-9 at day 3. ALP expression induced by cmRNA-encoding BMP-9 was significantly higher than the group transfected with cmRNA-encoding BMP-2. This result suggests that *BMP-9*-cmRNA had a more potent capacity to promote osteogenesis than *BMP-2*-cmRNA. The results showing the enhanced ALP activity were supported by findings by other groups where it was shown that increasing the activity of ALP in osteoprogenitor cells and osteoclasts had a positive feedback on formation of trabecular bone (14).

Effect of BMP-9-cmRNA and BMP-2-cmRNA on Calcium Deposition

Calcium salt sedimentation is a later stage marker for osteogenic differentiation (28). Alizarin red staining and atomic absorption spectroscopy were carried out at day 14 after transfection to investigate calcium salt sedimentation. Qualitative analysis showed higher calcium salt sedimentation by BMSCs transfected with *BMP-9*-cmRNA compared to BMSCs transfected with *BMP-2*-cmRNA. The greater the amount of mineralization, the stronger the staining with alizarin red. Qualitative assessment of alizarin red staining, as can be visualized in Fig. 3, indicated that *BMP-9*-cmRNA

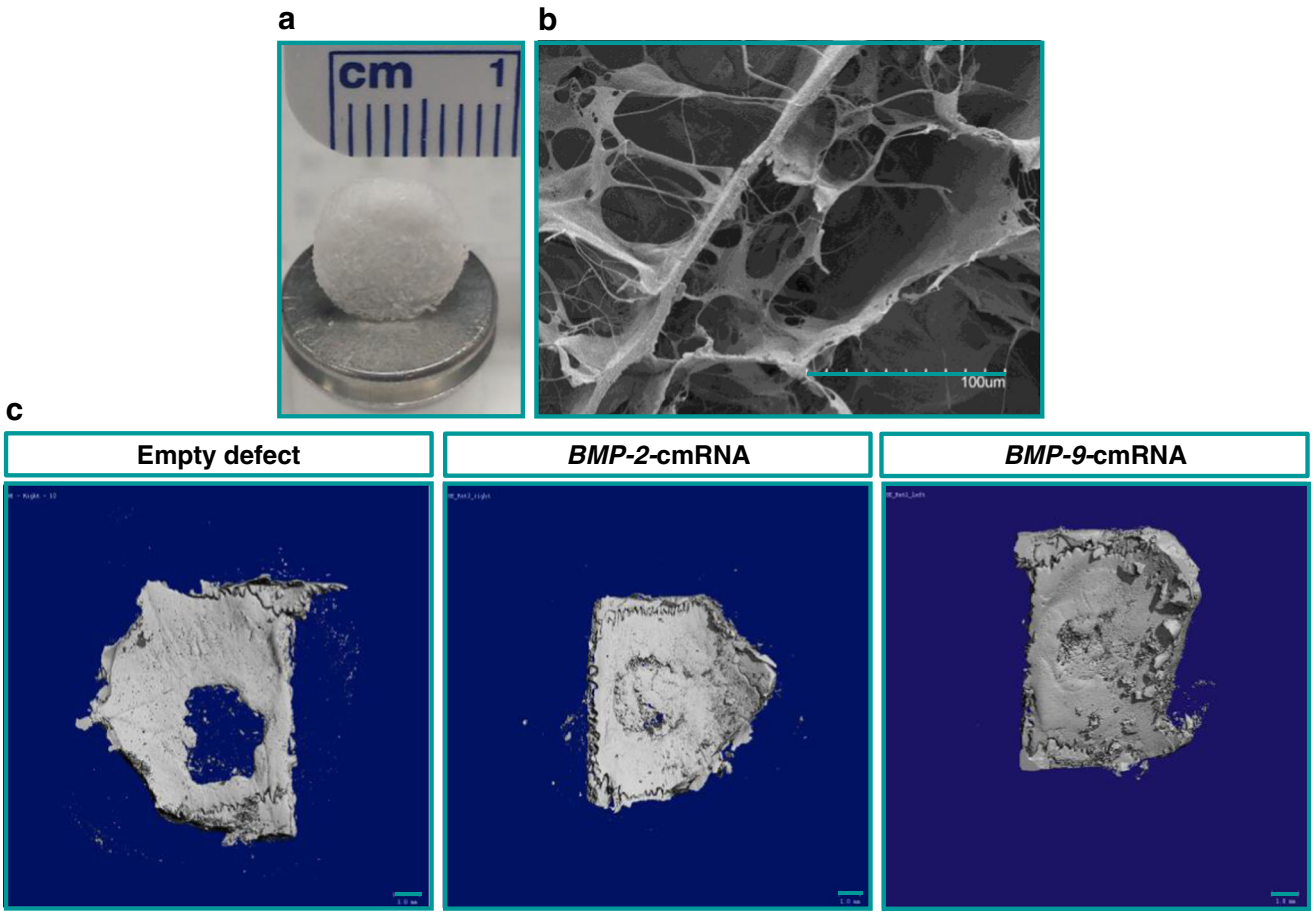

Fig. 5. Digital (**a**) and SEM (**b**) images of empty collagen scaffolds. *Scale bar*, 100 μm. Qualitative evaluation of *in vivo* bone repair (**c**); Representative μCT sagittal slices through calvarial defects showing the level of bone tissue regeneration after 4 weeks of treatment with different groups. *Scale bar*, 1 mm

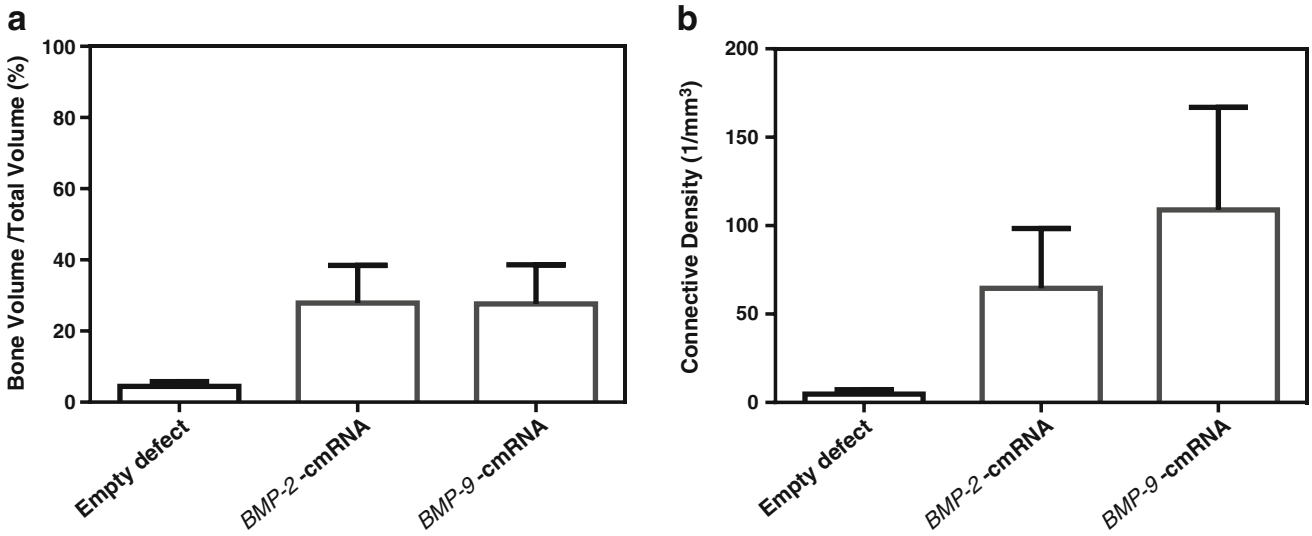

Fig. 6. Quantitative assessment of *in vivo* bone repair. **a** Bone volume fraction and **b** connectivity density in defects treated with empty defects ($n = 6$), scaffolds embedded with *BMP-2*-cmRNA ($n = 6$), and scaffolds embedded with *BMP-9*-cmRNA ($n = 6$). Values are expressed as mean ± SEM. No statistically significant differences were observed among the groups

promoted higher mineral deposition by BMSCs than did *BMP-2*-cmRNA or no treatment.

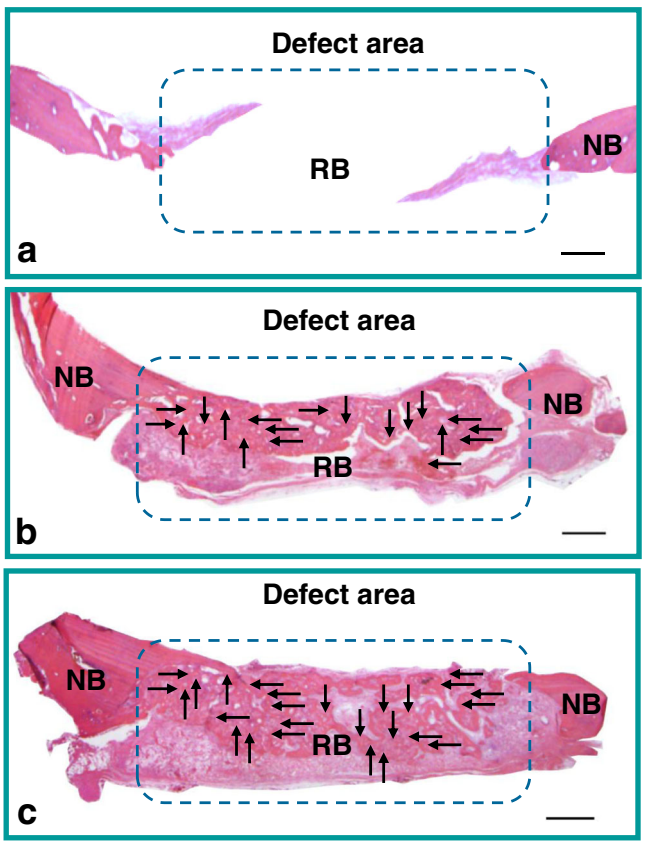

Fig. 7. Representative histology sections indicating the degree of new bone formation at the defect sites at 4 weeks, in response to **a** empty defect, **b** scaffolds embedded with *BMP-2*-cmRNA, and **c** scaffolds embedded with *BMP-9*-cmRNA. NB-native bone and RB-regenerated bone. The complete bridging of new bone is indicated by the *arrows*. *Scale bar*, 50 μm

Calcium deposition by BMSCs was quantified 14 days after transfection using an atomic absorption spectrophotometer. The *BMP-9*-cmRNA-treated group showed significantly higher levels of calcium salt sedimentation compared to the group receiving *BMP-2*-cmRNA as well as the control group (untreated BMSCs) (p value < 0.0001, Tukey's multiple comparison post-test) (Fig. 4.). In addition, cells transfected with *BMP-2*-cmRNA complexes revealed that there was a significant increase in calcium deposition compared to the control group (p value < 0.001, Tukey's multiple comparison post-test). These results suggest that *BMP-9*-cmRNA has a greater ability to stimulate calcium salt deposition in BMSCs, and was therefore a more efficient osteoinductive factor compared to *BMP-2*-cmRNA.

Degree of Bone Regeneration in Presence of BMP-9-cmRNA *Versus* BMP-2-cmRNA

Using critical size calvarial bone defects in a rat model, the effect of collagen matrices containing *BMP-9*-cmRNA or *BMP-2*-cmRNA on osteogenesis was investigated *in vivo*. The digital and SEM images of the utilized collagen matrix is shown in Fig. 5a and b. The *in vivo* efficacy of the following groups was investigated: (1) defects filled with *BMP-9*-cmRNA (50 μg) entrapped in collagen matrices, (2) defects filled with *BMP-2*-cmRNA (50 μg) entrapped in collagen matrices, and (3) empty defects. The rats were sacrificed after 4 weeks, the areas of interest were excised from the calvarial bone, and newly formed bone tissue was assessed for its volume and connectivity density using micro-computed tomography (μCT) scans.

Qualitative assessment of μCT images revealed an increase in callus formation in groups treated with either *BMP-9*-cmRNA- or *BMP-2*-cmRNA-loaded collagen matrices, compared to the control group (empty defect) (Fig. 5c.). Quantitative investigation of μCT scans of the regenerated bone was used to report the average bone volumes (fraction of regenerated bone volume to the total tissue volume of interest (BV/TV)) and connectivity density. The distribution

of BV/TV of defects treated with *BMP-9*-cmRNA or *BMP-2*-cmRNA was more than 6-fold higher compared to empty defects, albeit not significantly. There was no notable difference between the total bone volume of the *BMP-9*-cmRNA group and the *BMP-2*-cmRNA group (Fig. 6a). However, consistent with the increases observed in expression of ALP, alizarin red staining and Ca^{2+} salt sedimentation, the connectivity density of the regenerated bone was 2-fold greater for the group that received *BMP-9*-cmRNA compared to the *BMP-2*-cmRNA-treated group (Fig. 6b). Accordingly, a trend toward higher connectivity density was observed in the *BMP-9*-cmRNA-treated defects (23-fold increase) and *BMP-2*-cmRNA-treated defects (14-fold increase), when compared to the control group. The treatment groups were selected based on findings from our previous research where collagen scaffolds alone failed to regenerate bone in critical size rat calvarial defects (29). To check whether the non-significant results were due to a lack of statistical power, we conducted a post hoc power analysis using the SAS system with power $(1\text{-}\beta)$ set at 0.80 and $\alpha = 0.05$, two-tailed. The power for the BV/TV was computed to be 0.3, and for the connectivity, density was computed to be 0.09. This indicated that sample sizes would have to increase up to $n = 17$ and 94 for BV/TV and connectivity density, respectively, in order for group differences to reach statistical significance at the 0.05 level. Thus, non-significant results presented here can be attributed to a limited sample size.

These results on bone formation were verified by histology images stained with H & E. There was remarkably more mineralized regenerated bone tissue connecting the defect to the native bone in both the *BMP-9*-cmRNA treated, and *BMP-2*-cmRNA treated, groups relative to the control group. There was no evidence of bone formation in the control group. Figure 7 shows representative pictures of histology sections showing the degree of new bone formation. In the histomorphometric analysis that was performed on this particular example, more bone tissue formation was found in the *BMP-9*-cmRNA-treated group (with $37.7\% \pm 4.7$ bone regenerated area) compared to the *BMP-2*-cmRNA-treated group (with $18.6\% \pm 4.0$ bone regenerated area) and empty defect (with $2.81\% \pm 1.2$ bone regenerated area).

In the bone healing process, BMP-9 and BMP-2 signaling are involved in osteoid formation which leads to bone matrix mineralization and bone regeneration (30). We can assume that cmRNA is released from collagen matrices gradually to transfect nearby cells. Although μCT investigation and, to a lesser extent, histology data suggested that *BMP-9*-cmRNA has a greater capacity to induce osteogenesis, a larger sample size *in vivo* is required to achieve statistically significant data and thereby further validate the true bone regenerative properties of *BMP-9*-cmRNA compared to *BMP-2*-cmRNA.

CONCLUSION

In summary, the results from the present study revealed that *BMP-9*-cmRNA significantly enhanced osteogenic differentiation of BMSCs compared to *BMP-2*-cmRNA *in vitro*, as witnessed by upregulation of ALP expression, darker alizarin red staining, and demonstration of a more potent capacity to stimulate calcium mineralization. *In vivo*, the μCT and histology results demonstrated a trend toward higher bone connectivity density in calvarial defects treated with *BMP-9*-cmRNA-embedded collagen matrices when compared to the treatment containing *BMP-2*-cmRNA-embedded collagen matrices. These results show a trend where *BMP-9*-cmRNA was a more efficient osteoinductive factor in comparison with *BMP-2*-cmRNA. These findings suggest that *BMP-9*-cmRNA loaded into collagen matrices has the potential to be utilized for bone regeneration and has significant potential for bone repair in the clinic.

ACKNOWLEDGEMENTS

This study was supported by an NIH R21 grant (1R21DE024206-01A1), the University of Iowa Start-up Grant, the ITI Foundation for the Promotion of Implantology, Switzerland (ITI Research Grant No. 855 2012), the Osteology Foundation Grant (12–054), the Sunstar—American Academy of Periodontology Foundation Research Fellowship, and the Lyle and Sharon Bighley Professorship. The authors would like to thank Ryan D. Ross and Rick Sumner for their assistance in obtaining MicroCT images. Rush University Medical Center MicroCT/Histology Core resources were used. We also would like to thank Chantal Allamargot for technical support with histological image acquisition. Imaging equipment at the University of Iowa Core Microscopy Research Facility was used.

REFERENCES

1. Wright NC, Looker AC, Saag KG, Curtis JR, Delzell ES, Randall S, *et al*. The recent prevalence of osteoporosis and low bone mass in the United States based on bone mineral density at the femoral neck or lumbar spine. J Bone Miner Res. 2014;29:2520–6.
2. DeWitt N. Bone and cartilage. Nature. 2003;423:315.
3. Griffith LG, Naughton G. Tissue engineering—current challenges and expanding opportunities. Science. 2002;295:1009.
4. Kang Q, Sun MH, Cheng H, Peng Y, Montag AG, Deyrup AT, *et al*. Characterization of the distinct orthotopic bone-forming activity of 14 B.P. using recombinant adenovirus-mediated gene delivery. Gene Ther. 2004;11:1312–20.
5. Yang J, Shi P, Tu M, Wang Y, Liu M, Fan F, *et al*. Bone morphogenetic proteins: relationship between molecular structure and their osteogenic activity. Food Scie Human Wellness. 2014;3:127–35.
6. Riew KD, Wright NM, Cheng S, Avioli LV, Lou J. Induction of bone formation using a recombinant adenoviral vector carrying the human BMP-2 gene in a rabbit spinal fusion model. Calcif Tissue Int. 1998;63:357–60.
7. Sandhu HS, Khan SN, Suh DY, Boden SD. Demineralized bone matrix, bone morphogenetic proteins, and animal models of spine fusion: an overview. Eur Spine J. 2001;10 Suppl 2:S122–31.
8. M.P. Bostrom, N.P. Camacho, Potential role of bone morphogenetic proteins in fracture healing, Clin. Orthop. Relat. Res., (1998) S274-282
9. Bessa PC, Casal M, Reis RL. Bone morphogenetic proteins in tissue engineering: the road from the laboratory to the clinic, part I (basic concepts). J Tissue Eng Regen Med. 2008;2:1–13.
10. Fujioka-Kobayashi M, Sawada K, Kobayashi E, Schaller B, Zhang Y, Miron RJ. Recombinant human bone morphogenetic protein 9 (rhBMP9) induced osteoblastic behavior on a collagen membrane compared with rhBMP2. J Periodontol. 2016;87:e101–7.
11. Nohe A, Keating E, Knaus P, Petersen NO. Signal transduction of bone morphogenetic protein receptors. Cell Signal. 2004;16:291–9.

12. Kawabata M, Chytil A, Moses HL. Cloning of a novel type II serine/threonine kinase receptor through interaction with the type I transforming growth factor-β receptor. J Biol Chem. 1995;270:5625–30.
13. Heldin CH, Moustakas A. Role of Smads in TGFbeta signaling. Cell Tissue Res. 2012;347:21–36.
14. Cheng H, Jiang W, Phillips FM, Haydon RC, Peng Y, Zhou L, *et al*. Osteogenic activity of the fourteen types of human bone morphogenetic proteins (BMPs). J Bone Joint Surg Am. 2003;85-a:1544–52.
15. Peng Y, Kang Q, Luo Q, Jiang W, Si W, Liu BA, *et al*. Inhibitor of DNA binding/differentiation helix-loop-helix proteins mediate bone morphogenetic protein-induced osteoblast differentiation of mesenchymal stem cells. J Biol Chem. 2004;279:32941–9.
16. Wang Y, Hong S, Li M, Zhang J, Bi Y, He Y, *et al*. Noggin resistance contributes to the potent osteogenic capability of BMP9 in mesenchymal stem cells. J Orthop Res. 2013;31:1796–803.
17. Kirsch T, Sebald W, Dreyer MK. Crystal structure of the BMP-2-BRIA ectodomain complex. Nat Struct Biol. 2000;7:492–6.
18. Brown MA, Zhao Q, Baker KA, Naik C, Chen C, Pukac L, *et al*. Crystal structure of BMP-9 and functional interactions with pro-region and receptors. J Biol Chem. 2005;280:25111–8.
19. Lamplot JD, Qin J, Nan G, Wang J, Liu X, Yin L, *et al*. BMP9 signaling in stem cell differentiation and osteogenesis. American J Stem Cells. 2013;2:1–21.
20. Winn SR, Hu Y, Sfeir C, Hollinger JO. Gene therapy approaches for modulating bone regeneration. Adv Drug Deliv Rev. 2000;42:121–38.
21. Carragee EJ, Chu G, Rohatgi R, Hurwitz EL, Weiner BK, Yoon ST, *et al*. Cancer risk after use of recombinant bone morphogenetic protein-2 for spinal arthrodesis. J Bone Joint Surg Am. 2013;95:1537–45.
22. Elangovan S, Khorsand B, Do A-V, Hong L, Dewerth A, Kormann M, *et al*. Chemically modified RNA activated matrices enhance bone regeneration. J Control Release. 2015;218:22–8.
23. Balmayor ER, Geiger JP, Aneja MK, Berezhanskyy T, Utzinger M, Mykhaylyk O, *et al*. Chemically modified RNA induces osteogenesis of stem cells and human tissue explants as well as accelerates bone healing in rats. Biomaterials. 2016;87:131–46.
24. Kormann MSD, Hasenpusch G, Aneja MK, Nica G, Flemmer AW, Herber-Jonat S, *et al*. Expression of therapeutic proteins after delivery of chemically modified mRNA in mice. Nat Biotechnol. 2011;29:154–7.
25. Holtkamp S, Kreiter S, Selmi A, Simon P, Koslowski M, Huber C, *et al*. Modification of antigen-encoding RNA increases stability, translational efficacy, and T-cell stimulatory capacity of dendritic cells. Blood. 2006;108:4009.
26. Elangovan S, D'Mello SR, Hong L, Ross RD, Allamargot C, Dawson DV, *et al*. The enhancement of bone regeneration by gene activated matrix encoding for platelet derived growth factor. Biomaterials. 2014;35:737–47.
27. Xu DJ, Zhao YZ, Wang J, He JW, Weng YG, Luo JY. Smads, p38 and ERK1/2 are involved in BMP9-induced osteogenic differentiation of C3H10T1/2 mesenchymal stem cells. BMB Rep. 2012;45:247–52.
28. Birmingham E, Niebur GL, McHugh PE, Shaw G, Barry FP, McNamara LM. Osteogenic differentiation of mesenchymal stem cells is regulated by osteocyte and osteoblast cells in a simplified bone niche. Eur Cell Mater. 2012;23:13–27.
29. D'Mello SR, Elangovan S, Hong L, Ross RD, Sumner DR, Salem AK. A pilot study evaluating combinatorial and simultaneous delivery of Polyethylenimine-plasmid DNA complexes encoding for VEGF and PDGF for bone regeneration in calvarial bone defects. Curr Pharm Biotechnol. 2015;16:655–60.
30. Seib FP, Franke M, Jing D, Werner C, Bornhäuser M. Endogenous bone morphogenetic proteins in human bone marrow-derived multipotent mesenchymal stromal cells. Eur J Cell Biol. 2009;88:257–71.